



CHORUS

This is the accepted manuscript made available via CHORUS. The article has been published as:

Precision measurement of the D^{*0} decay branching fractions

M. Ablikim *et al.* (BESIII Collaboration)

Phys. Rev. D **91**, 031101 — Published 6 February 2015

DOI: [10.1103/PhysRevD.91.031101](https://doi.org/10.1103/PhysRevD.91.031101)

Precision measurement of the D^{*0} decay branching fractions

M. Ablikim¹, M. N. Achasov^{8,a}, X. C. Ai¹, O. Albayrak⁴, M. Albrecht³, D. J. Ambrose⁴³, A. Amoroso^{47A,47C}, F. F. An¹, Q. An⁴⁴, J. Z. Bai¹, R. Baldini Ferroli^{19A}, Y. Ban³⁰, D. W. Bennett¹⁸, J. V. Bennett⁴, M. Bertani^{19A}, D. Bettoni^{20A}, J. M. Bian⁴², F. Bianchi^{47A,47C}, E. Boger^{22,h}, O. Bondarenko²⁴, I. Boyko²², R. A. Briere⁴, H. Cai⁴⁹, X. Cai¹, O. Cakir^{39A,b}, A. Calcaterra^{19A}, G. F. Cao¹, S. A. Cetin^{39B}, J. F. Chang¹, G. Chelkov^{22,c}, G. Chen¹, H. S. Chen¹, H. Y. Chen², J. C. Chen¹, M. L. Chen¹, S. J. Chen²⁸, X. Chen¹, X. R. Chen²⁵, Y. B. Chen¹, H. P. Cheng¹⁶, X. K. Chu³⁰, G. Cibinetto^{20A}, D. Cronin-Hennessy⁴², H. L. Dai¹, J. P. Dai³³, A. Dbeysi¹³, D. Dedovich²², Z. Y. Deng¹, A. Denig²¹, I. Denysenko²², M. Destefanis^{47A,47C}, F. De Mori^{47A,47C}, Y. Ding²⁶, C. Dong²⁹, J. Dong¹, L. Y. Dong¹, M. Y. Dong¹, S. X. Du⁵¹, P. F. Duan¹, J. Z. Fan³⁸, J. Fang¹, S. S. Fang¹, X. Fang⁴⁴, Y. Fang¹, L. Fava^{47B,47C}, F. Feldbauer²¹, G. Felici^{19A}, C. Q. Feng⁴⁴, E. Fioravanti^{20A}, M. Fritsch^{13,21}, C. D. Fu¹, Q. Gao¹, Y. Gao³⁸, I. Garzia^{20A}, K. Goetzen⁹, W. X. Gong¹, W. Gradl²¹, M. Greco^{47A,47C}, M. H. Gu¹, Y. T. Gu¹¹, Y. H. Guan¹, A. Q. Guo¹, L. B. Guo²⁷, T. Guo²⁷, Y. Guo¹, Y. P. Guo²¹, Z. Haddadi²⁴, A. Hafner²¹, S. Han⁴⁹, Y. L. Han¹, F. A. Harris⁴¹, K. L. He¹, Z. Y. He²⁹, T. Held³, Y. K. Heng¹, Z. L. Hou¹, C. Hu²⁷, H. M. Hu¹, J. F. Hu^{47A}, T. Hu¹, Y. Hu¹, G. M. Huang⁵, G. S. Huang⁴⁴, H. P. Huang⁴⁹, J. S. Huang¹⁴, X. T. Huang³², Y. Huang²⁸, T. Hussain⁴⁶, Q. Ji¹, Q. P. Ji²⁹, X. B. Ji¹, X. L. Ji¹, L. L. Jiang¹, L. W. Jiang⁴⁹, X. S. Jiang¹, J. B. Jiao³², Z. Jiao¹⁶, D. P. Jin¹, S. Jin¹, T. Johansson⁴⁸, A. Julin⁴², N. Kalantar-Nayestanaki²⁴, X. L. Kang¹, X. S. Kang²⁹, M. Kavatsyuk²⁴, B. C. Ke⁴, R. Kliemt¹³, B. Kloss²¹, O. B. Kolcu^{39B,d}, B. Kopf³, M. Kornicer⁴¹, W. Kuehn²³, A. Kupsc⁴⁸, W. Lai¹, J. S. Lange²³, M. Lara¹⁸, P. Larin¹³, C. H. Li¹, Cheng Li⁴⁴, D. M. Li⁵¹, F. Li¹, G. Li¹, H. B. Li¹, J. C. Li¹, Jin Li³¹, K. Li¹², K. Li³², P. R. Li⁴⁰, T. Li³², W. D. Li¹, W. G. Li¹, X. L. Li³², X. M. Li¹¹, X. N. Li¹, X. Q. Li²⁹, Z. B. Li³⁷, H. Liang⁴⁴, Y. F. Liang³⁵, Y. T. Liang²³, G. R. Liao¹⁰, D. X. Lin¹³, B. J. Liu¹, C. L. Liu⁴, C. X. Liu¹, F. H. Liu³⁴, Fang Liu¹, Feng Liu⁵, H. B. Liu¹¹, H. H. Liu¹, H. H. Liu¹⁵, H. M. Liu¹, J. Liu¹, J. P. Liu⁴⁹, J. Y. Liu¹, K. Liu³⁸, K. Y. Liu²⁶, L. D. Liu³⁰, P. L. Liu¹, Q. Liu⁴⁰, S. B. Liu⁴⁴, X. Liu²⁵, X. X. Liu⁴⁰, Y. B. Liu²⁹, Z. A. Liu¹, Zhiqiang Liu¹, Zhiqing Liu²¹, H. Loehner²⁴, X. C. Lou^{1,e}, H. J. Lu¹⁶, J. G. Lu¹, R. Q. Lu¹⁷, Y. Lu¹, Y. P. Lu¹, C. L. Luo²⁷, M. X. Luo⁵⁰, T. Luo⁴¹, X. L. Luo¹, M. Lv¹, X. R. Lyu⁴⁰, F. C. Ma²⁶, H. L. Ma¹, L. L. Ma³², Q. M. Ma¹, S. Ma¹, T. Ma¹, X. N. Ma²⁹, X. Y. Ma¹, F. E. Maas¹³, M. Maggiora^{47A,47C}, Q. A. Malik⁴⁶, Y. J. Mao³⁰, Z. P. Mao¹, S. Marcello^{47A,47C}, J. G. Messchendorp²⁴, J. Min¹, T. J. Min¹, R. E. Mitchell¹⁸, X. H. Mo¹, Y. J. Mo⁵, C. Morales Morales¹³, K. Moriya¹⁸, N. Yu. Muchnoi^{8,a}, H. Muramatsu⁴², Y. Nefedov²², F. Nerling¹³, I. B. Nikolaev^{8,a}, Z. Ning¹, S. Nisar⁷, S. L. Niu¹, X. Y. Niu¹, S. L. Olsen³¹, Q. Ouyang¹, S. Pacetti^{19B}, P. Patteri^{19A}, M. Pelizaeus³, H. P. Peng⁴⁴, K. Peters⁹, J. L. Ping²⁷, R. G. Ping¹, R. Poling⁴², Y. N. Pu¹⁷, M. Qi²⁸, S. Qian¹, C. F. Qiao⁴⁰, L. Q. Qin³², N. Qin⁴⁹, X. S. Qin¹, Y. Qin³⁰, Z. H. Qin¹, J. F. Qiu¹, K. H. Rashid⁴⁶, C. F. Redmer²¹, H. L. Ren¹⁷, M. Ripka²¹, G. Rong¹, X. D. Ruan¹¹, V. Santoro^{20A}, A. Sarantsev^{22,f}, M. Savrie^{20B}, K. Schoenning⁴⁸, S. Schumann²¹, W. Shan³⁰, M. Shao⁴⁴, C. P. Shen², P. X. Shen²⁹, X. Y. Shen¹, H. Y. Sheng¹, M. R. Shepherd¹⁸, W. M. Song¹, X. Y. Song¹, S. Sosio^{47A,47C}, S. Spataro^{47A,47C}, B. Spruck²³, G. X. Sun¹, J. F. Sun¹⁴, S. S. Sun¹, Y. J. Sun⁴⁴, Y. Z. Sun¹, Z. J. Sun¹, Z. T. Sun¹⁸, C. J. Tang³⁵, X. Tang¹, I. Tapan^{39C}, E. H. Thorndike⁴³, M. Tiemens²⁴, D. Toth⁴², M. Ullrich²³, I. Uman^{39B}, G. S. Varner⁴¹, B. Wang²⁹, B. L. Wang⁴⁰, D. Wang³⁰, D. Y. Wang³⁰, K. Wang¹, L. L. Wang¹, L. S. Wang¹, M. Wang³², P. Wang¹, P. L. Wang¹, Q. J. Wang¹, S. G. Wang³⁰, W. Wang¹, X. F. Wang³⁸, Y. D. Wang^{19A}, Y. F. Wang¹, Y. Q. Wang²¹, Z. Wang¹, Z. G. Wang¹, Z. H. Wang⁴⁴, Z. Y. Wang¹, T. Weber²¹, D. H. Wei¹⁰, J. B. Wei³⁰, P. Weidenkaff²¹, S. P. Wen¹, U. Wiedner³, M. Wolke⁴⁸, L. H. Wu¹, Z. Wu¹, L. G. Xia³⁸, Y. Xia¹⁷, D. Xiao¹, Z. J. Xiao²⁷, Y. G. Xie¹, G. F. Xu¹, L. Xu¹, Q. J. Xu¹², Q. N. Xu⁴⁰, X. P. Xu³⁶, L. Yan⁴⁴, W. B. Yan⁴⁴, W. C. Yan⁴⁴, Y. H. Yan¹⁷, H. X. Yang¹, L. Yang⁴⁹, Y. Yang⁵, Y. X. Yang¹⁰, H. Ye¹, M. Ye¹, M. H. Ye⁶, J. H. Yin¹, B. X. Yu¹, C. X. Yu²⁹, H. W. Yu³⁰, J. S. Yu²⁵, C. Z. Yuan¹, W. L. Yuan²⁸, Y. Yuan¹, A. Yuncu^{39B,g}, A. A. Zafar⁴⁶, A. Zallo^{19A}, Y. Zeng¹⁷, B. X. Zhang¹, B. Y. Zhang¹, C. Zhang²⁸, C. C. Zhang¹, D. H. Zhang¹, H. H. Zhang³⁷, H. Y. Zhang¹, J. J. Zhang¹, J. L. Zhang¹, J. Q. Zhang¹, J. W. Zhang¹, J. Y. Zhang¹, J. Z. Zhang¹, K. Zhang¹, L. Zhang¹, S. H. Zhang¹, X. J. Zhang¹, X. Y. Zhang³², Y. Zhang¹, Y. H. Zhang¹, Z. H. Zhang⁵, Z. P. Zhang⁴⁴, Z. Y. Zhang⁴⁹, G. Zhao¹, J. W. Zhao¹, J. Y. Zhao¹, J. Z. Zhao¹, Lei Zhao⁴⁴, Ling Zhao¹, M. G. Zhao²⁹, Q. Zhao¹, Q. W. Zhao¹, S. J. Zhao⁵¹, T. C. Zhao¹, Y. B. Zhao¹, Z. G. Zhao⁴⁴, A. Zhemchugov^{22,h}, B. Zheng⁴⁵, J. P. Zheng¹, W. J. Zheng³², Y. H. Zheng⁴⁰, B. Zhong²⁷, L. Zhou¹, Li Zhou²⁹, X. Zhou⁴⁹, X. K. Zhou⁴⁴, X. R. Zhou⁴⁴, X. Y. Zhou¹, K. Zhu¹, K. J. Zhu¹, S. Zhu¹, X. L. Zhu³⁸, Y. C. Zhu⁴⁴, Y. S. Zhu¹, Z. A. Zhu¹, J. Zhuang¹, B. S. Zou¹, J. H. Zou¹

(BESIII Collaboration)

¹ Institute of High Energy Physics, Beijing 100049, People's Republic of China

² Beihang University, Beijing 100191, People's Republic of China

³ Bochum Ruhr-University, D-44780 Bochum, Germany

⁴ Carnegie Mellon University, Pittsburgh, Pennsylvania 15213, USA

⁵ Central China Normal University, Wuhan 430079, People's Republic of China

⁶ China Center of Advanced Science and Technology, Beijing 100190, People's Republic of China

⁷ COMSATS Institute of Information Technology, Lahore, Defence Road, Off Raiwind Road, 54000 Lahore, Pakistan

⁸ G.I. Budker Institute of Nuclear Physics SB RAS (BINP), Novosibirsk 630090, Russia

⁹ GSI Helmholtzcentre for Heavy Ion Research GmbH, D-64291 Darmstadt, Germany

¹⁰ Guangxi Normal University, Guilin 541004, People's Republic of China

¹¹ GuangXi University, Nanning 530004, People's Republic of China

¹² Hangzhou Normal University, Hangzhou 310036, People's Republic of China

¹³ Helmholtz Institute Mainz, Johann-Joachim-Becher-Weg 45, D-55099 Mainz, Germany

¹⁴ Henan Normal University, Xinxiang 453007, People's Republic of China

- ¹⁵ Henan University of Science and Technology, Luoyang 471003, People's Republic of China
- ¹⁶ Huangshan College, Huangshan 245000, People's Republic of China
- ¹⁷ Hunan University, Changsha 410082, People's Republic of China
- ¹⁸ Indiana University, Bloomington, Indiana 47405, USA
- ¹⁹ (A)INFN Laboratori Nazionali di Frascati, I-00044, Frascati, Italy; (B)INFN and University of Perugia, I-06100, Perugia, Italy
- ²⁰ (A)INFN Sezione di Ferrara, I-44122, Ferrara, Italy; (B)University of Ferrara, I-44122, Ferrara, Italy
- ²¹ Johannes Gutenberg University of Mainz, Johann-Joachim-Becher-Weg 45, D-55099 Mainz, Germany
- ²² Joint Institute for Nuclear Research, 141980 Dubna, Moscow region, Russia
- ²³ Justus Liebig University Giessen, II. Physikalisches Institut, Heinrich-Buff-Ring 16, D-35392 Giessen, Germany
- ²⁴ KVI-CART, University of Groningen, NL-9747 AA Groningen, The Netherlands
- ²⁵ Lanzhou University, Lanzhou 730000, People's Republic of China
- ²⁶ Liaoning University, Shenyang 110036, People's Republic of China
- ²⁷ Nanjing Normal University, Nanjing 210023, People's Republic of China
- ²⁸ Nanjing University, Nanjing 210093, People's Republic of China
- ²⁹ Nankai University, Tianjin 300071, People's Republic of China
- ³⁰ Peking University, Beijing 100871, People's Republic of China
- ³¹ Seoul National University, Seoul, 151-747 Korea
- ³² Shandong University, Jinan 250100, People's Republic of China
- ³³ Shanghai Jiao Tong University, Shanghai 200240, People's Republic of China
- ³⁴ Shanxi University, Taiyuan 030006, People's Republic of China
- ³⁵ Sichuan University, Chengdu 610064, People's Republic of China
- ³⁶ Soochow University, Suzhou 215006, People's Republic of China
- ³⁷ Sun Yat-Sen University, Guangzhou 510275, People's Republic of China
- ³⁸ Tsinghua University, Beijing 100084, People's Republic of China
- ³⁹ (A)Istanbul Aydin University, 34295 Sefakoy, Istanbul, Turkey; (B)Dogus University, 34722 Istanbul, Turkey; (C)Uludag University, 16059 Bursa, Turkey
- ⁴⁰ University of Chinese Academy of Sciences, Beijing 100049, People's Republic of China
- ⁴¹ University of Hawaii, Honolulu, Hawaii 96822, USA
- ⁴² University of Minnesota, Minneapolis, Minnesota 55455, USA
- ⁴³ University of Rochester, Rochester, New York 14627, USA
- ⁴⁴ University of Science and Technology of China, Hefei 230026, People's Republic of China
- ⁴⁵ University of South China, Hengyang 421001, People's Republic of China
- ⁴⁶ University of the Punjab, Lahore-54590, Pakistan
- ⁴⁷ (A)University of Turin, I-10125, Turin, Italy; (B)University of Eastern Piedmont, I-15121, Alessandria, Italy; (C)INFN, I-10125, Turin, Italy
- ⁴⁸ Uppsala University, Box 516, SE-75120 Uppsala, Sweden
- ⁴⁹ Wuhan University, Wuhan 430072, People's Republic of China
- ⁵⁰ Zhejiang University, Hangzhou 310027, People's Republic of China
- ⁵¹ Zhengzhou University, Zhengzhou 450001, People's Republic of China
- ^a Also at the Novosibirsk State University, Novosibirsk, 630090, Russia
- ^b Also at Ankara University, 06100 Tandogan, Ankara, Turkey
- ^c Also at the Moscow Institute of Physics and Technology, Moscow 141700, Russia and at the Functional Electronics Laboratory, Tomsk State University, Tomsk, 634050, Russia
- ^d Currently at Istanbul Arel University, Kucukcekmece, Istanbul, Turkey
- ^e Also at University of Texas at Dallas, Richardson, Texas 75083, USA
- ^f Also at the PNPI, Gatchina 188300, Russia
- ^g Also at Bogazici University, 34342 Istanbul, Turkey
- ^h Also at the Moscow Institute of Physics and Technology, Moscow 141700, Russia

Using 482 pb⁻¹ of data taken at $\sqrt{s} = 4.009$ GeV, we measure the branching fractions of the decays of D^{*0} into $D^0\pi^0$ and $D^0\gamma$ to be $\mathcal{B}(D^{*0} \rightarrow D^0\pi^0) = (65.5 \pm 0.8 \pm 0.5)\%$ and $\mathcal{B}(D^{*0} \rightarrow D^0\gamma) = (34.5 \pm 0.8 \pm 0.5)\%$ respectively, by assuming that the D^{*0} decays only into these two modes. The ratio of the two branching fractions is $\mathcal{B}(D^{*0} \rightarrow D^0\pi^0)/\mathcal{B}(D^{*0} \rightarrow D^0\gamma) = 1.90 \pm 0.07 \pm 0.05$, which is independent of the assumption made above. The first uncertainties are statistical and the second ones systematic. The precision is improved by a factor of three compared to the present world average values.

PACS numbers: 13.20.Fc, 13.25.Ft, 14.40.Lb

I. INTRODUCTION

In the framework of QCD, the building blocks of matter,

colored quarks, interact with each other by exchanging $SU(3)$ Yang-Mills gauge bosons, gluons, which are also colored. Consequently, the quark-gluon dynamics becomes nonperturbative in the low energy regime. Many effective models (EMs), such as the potential model, heavy quark and chiral symmetries, and QCD sum rules, have been developed to deal with the nonperturbative effects, as described in a recent review [2]. The charmed meson, described as a hydrogen-like hadronic system consisting of a heavy quark (c quark) and a light quark (u , d , or s quark), is a particularly suited laboratory to test the EMs mentioned above. The decay branching fractions of D^{*0} to $D^0\pi^0$ (hadronic decay) and $D^0\gamma$ (radiative decay) have been studied by a number of authors based on EMs [3–6]. A precise measurement of the branching fractions will constrain the model parameters and thereby help to improve the EMs. On the experimental side, these two branching fractions are critical input values for many measurements such as the open charm cross section in e^+e^- annihilation [7] and the semileptonic decays of B^\pm [8].

These branching fractions have been measured in many electron-positron collision experiments, such as CLEO [9], ARGUS [10], BABAR [11] etc., but the uncertainties of the averaged branching fractions by the Particle Data Group (PDG) [12] are large (about 8%). The data sample used in this analysis of 482 pb^{-1} collected at a center-of-mass (CM) energy $\sqrt{s} = 4.009 \text{ GeV}$ with the BESIII detector provides an opportunity for significant improvement.

II. BESIII DETECTOR AND MONTE CARLO

BESIII is a general purpose detector which covers 93% of the solid angle, and operates at the e^+e^- collider BEPCII. Its construction is described in great detail in Ref. [13]. It consists of four main components: (a) A small-cell, helium-based main drift chamber (MDC) with 43 layers providing an average single-hit resolution of $135 \mu\text{m}$, and a momentum resolution of 0.5% for charged-particle at $1 \text{ GeV}/c$ in a 1 T magnetic field. (b) An electro-magnetic calorimeter (EMC) consisting of 6240 CsI(Tl) crystals in a cylindrical structure (barrel and two end-caps). The energy resolution for 1 GeV photons is 2.5% (5%) in the barrel (end-caps), while the position resolution is 6 mm (9 mm) in the barrel (end-caps). (c) A time-of-flight system (TOF), which is constructed of 5-cm-thick plastic scintillators and includes 88 detectors of 2.4 m length in two layers in the barrel and 96 fan-shaped detectors in the end-caps. The barrel (end-cap) time resolution of 80 ps (110 ps) provides 2σ K/π separation for momenta up to about $1 \text{ GeV}/c$. (d) The muon counter (MUC), consisting of Resistive Plate Chambers (RPCs) in nine barrel and eight end-cap layers, is incorporated in the return iron of the super-conducting magnet, and provides a position resolution of about 2 cm.

To investigate the event selection criteria, calculate the selection efficiency, and estimate the background, Monte Carlo (MC) simulated samples including 1,000,000 signal MC events and 500 pb^{-1} inclusive MC events are generated. The event generator KKMC [14] is used to generate the charmonium state including initial state radiation (ISR) and the beam energy spread; EVTGEN [15] is used to generate the charmonium decays with known branching ratios [12]; the unknown charmonium decays are generated based on the LUNDCHARM model [16]; and continuum events are generated with PYTHIA [17]. In simulating the ISR events, the $e^+e^- \rightarrow D^{*0}\bar{D}^0$ cross section measured with BESIII data at CM energies from threshold to 4.009 GeV is used as input. A GEANT4 [18, 19] based detector simulation package is used to model the detector response.

III. METHODOLOGY AND EVENT SELECTION

At $\sqrt{s} = 4.009 \text{ GeV}$, $e^+e^- \rightarrow D^{*0}\bar{D}^0 + c.c.$ is produced copiously. Assuming that there are only two decay modes for D^{*0} , i.e., $D^{*0} \rightarrow D^0\pi^0$ and $D^{*0} \rightarrow D^0\gamma$, the final states of $D^{*0}\bar{D}^0$ decays will be either $D^0\bar{D}^0\pi^0$ or $D^0\bar{D}^0\gamma$. Such an assumption is reasonable, since as shown in Ref. [20], the next largest branching fraction mode $D^{*0} \rightarrow D^0\gamma\gamma$ is expected to be less than 3.3×10^{-5} . The CM energy is not high enough for $D^{*0}\bar{D}^{*0}$ production. To select $e^+e^- \rightarrow D^{*0}\bar{D}^0$ signal events, we first reconstruct the $D^0\bar{D}^0$ pair, and then require that the mass recoiling against the $D^0\bar{D}^0$ system corresponds to a π^0 at its nominal mass [12] or a photon with a mass of zero. This approach allows us to measure the D^{*0} decay branching ratios from the numbers of $D^{*0} \rightarrow D^0\pi^0$ and $D^{*0} \rightarrow D^0\gamma$ events in the $D^0\bar{D}^0$ recoil mass spectra without reconstructing the π^0 or γ .

To increase the statistics and limit backgrounds, three D^0 decay modes with large branching fractions and simple topologies are used, as shown in Table I. The corresponding five combinations are labeled as modes I to V. Combinations with more than one π^0 or more than 6 charged tracks are not used in this analysis.

TABLE I. The charmed meson tag modes.

Mode	Decay of D^0	Decay of \bar{D}^0
I	$D^0 \rightarrow K^-\pi^+$	$\bar{D}^0 \rightarrow K^+\pi^-$
II	$D^0 \rightarrow K^-\pi^+$	$\bar{D}^0 \rightarrow K^+\pi^-\pi^0$
III	$D^0 \rightarrow K^-\pi^+\pi^0$	$\bar{D}^0 \rightarrow K^+\pi^-$
IV	$D^0 \rightarrow K^-\pi^+$	$\bar{D}^0 \rightarrow K^+\pi^-\pi^+\pi^-$
V	$D^0 \rightarrow K^-\pi^+\pi^+\pi^-$	$\bar{D}^0 \rightarrow K^+\pi^-$

To select a good charged track, we require that it must originate within 10 cm to the interaction point in

the beam direction and 1 cm in the plane perpendicular to the beam. In addition, a good charged track should be within $|\cos\theta| < 0.93$, where θ is its polar angle in the MDC. Information from the TOF and energy loss (dE/dx) measurements in the MDC are combined to form a probability P_π (P_K) with a pion (kaon) assumption. To identify a pion (kaon), the probability P_π (P_K) is required to be greater than 0.1%, and $P_\pi > P_K$ ($P_K > P_\pi$). In modes I-III, one oppositely charged kaon pair and one oppositely charged pion pair are required in the final state; while in modes IV and V, one oppositely charged kaon pair and two oppositely charged pion pairs are required.

Photons, which are reconstructed from isolated showers in the EMC, are required to be at least 20 degrees away from charged tracks and to have energy greater than 25 MeV in the barrel EMC or 50 MeV in the end-cap EMC. To suppress electronic noise and energy deposits unrelated to the signal event, the EMC time (t) of the photon candidate should be coincident with the collision event time, namely $0 \leq t \leq 700$ ns. We require at least two good photons in modes II and III.

In order to improve the resolution of the $D^0\bar{D}^0$ recoil mass, a kinematic fit is performed with the D^0 and \bar{D}^0 candidates constrained to the nominal D^0 mass [12]. In modes II and III, after requiring the invariant mass of the two photons be within ± 15 MeV/ c^2 of the nominal π^0 mass, a π^0 mass constraint is also included in the fit. The total χ^2 is calculated for the fit, and when there is more than one $D^0\bar{D}^0$ combinations satisfying the selection criteria above, the one with the least total χ^2 is selected. Figure 1 shows comparisons of some interesting distributions between MC simulation and data after applying the selection criteria above. Reasonable agreement between data and MC simulation is observed, and the differences are considered in the systematic uncertainty estimation. Figure 1(a) shows the total χ^2 distribution; χ^2 less than 30 is required to increase the purity of the signal. Figures 1(b) and 1(c) show the distributions of D^0 momentum and \bar{D}^0 momentum in the e^+e^- center-of-mass system. The small peaks at 0.75 GeV/ c are from direct $e^+e^- \rightarrow D^0\bar{D}^0$ production. To suppress such background events, we require that the momenta of both D^0 and \bar{D}^0 to be less than 0.65 GeV/ c . Another source of background events is ISR production of $\psi(3770)$ with subsequent decay $\psi(3770) \rightarrow D^0\bar{D}^0$, the number of which is obtained from MC simulation. As shown in Fig. 1(d), the right and left peaks in the distribution of the square of the $D^0\bar{D}^0$ recoil mass correspond to $D^{*0} \rightarrow D^0\pi^0$ and $D^{*0} \rightarrow D^0\gamma$ events respectively; the respective signal regions are defined by $[0.01, 0.04]$ and $[-0.01, 0.01]$ (GeV/ c^2)² in the further analysis.

IV. BRANCHING FRACTIONS

We calculate the branching fraction of $D^{*0} \rightarrow D^0\pi^0$ using $\mathcal{B}(D^{*0} \rightarrow D^0\pi^0) = \frac{N_{\pi^0}^{\text{prod}}}{N_\gamma^{\text{prod}} + N_{\pi^0}^{\text{prod}}}$, where N_γ^{prod} and $N_{\pi^0}^{\text{prod}}$ are the numbers of produced $D^{*0} \rightarrow D^0\gamma$ and $D^{*0} \rightarrow D^0\pi^0$ events, respectively, which are obtained by solving the following equations

$$\begin{pmatrix} N_{\pi^0}^{\text{obs}} - N_{\pi^0}^{\text{bkg}} \\ N_\gamma^{\text{obs}} - N_\gamma^{\text{bkg}} \end{pmatrix} = \begin{pmatrix} \epsilon_{\pi^0\pi^0} & \epsilon_{\gamma\pi^0} \\ \epsilon_{\pi^0\gamma} & \epsilon_{\gamma\gamma} \end{pmatrix} \begin{pmatrix} N_{\pi^0}^{\text{prod}} \\ N_\gamma^{\text{prod}} \end{pmatrix}, \quad (1)$$

where N_i^{obs} and N_i^{bkg} are the number of selected events in data and the number of background events estimated from MC simulation in the $D^{*0} \rightarrow D^0 + i$ mode, respectively; ϵ_{ij} is the efficiency of selecting the generated $D^{*0} \rightarrow D^0 + i$ events as $D^{*0} \rightarrow D^0 + j$, determined from MC simulation. Here, i and j denote π^0 or γ . In the simulation, all decay channels of the π^0 from D^{*0} decays are taken into account.

The numbers used in the calculation and the measured branching fractions are listed in Table II. For mode II and III, the final state used to reconstruct the charm meson contains a π^0 , so the efficiency for $D^{*0} \rightarrow D^0\pi^0$ will be higher when the π^0 outside the charm meson is misidentified as the π^0 from charm meson decays; for the other three modes, the efficiency difference is caused by the dividing line, this can be illustrated by the fact that $\epsilon_{\pi^0\pi^0} + \epsilon_{\pi^0\gamma}$ almost equals to $\epsilon_{\gamma\gamma} + \epsilon_{\gamma\pi^0}$. The results from each mode and their weighted average are shown in Fig. 2; the goodness of the fit determined with respect to the weighted average is $\chi^2/\text{n.d.f.} = 3.6/4$, which means that the results from these five modes are consistent with each other. Here n.d.f. is the number of degrees of freedom. The combined result ($\mathcal{B}(D^{*0} \rightarrow D^0\pi^0) = 65.7 \pm 0.8\%$), which is calculated by directly summing the number of events for the five modes together, is consistent with the weighted average ($\mathcal{B}(D^{*0} \rightarrow D^0\pi^0) = 65.5 \pm 0.8\%$). The weighted average is taken as the nominal result. A cross check is performed by fitting the square of the $D^0\bar{D}^0$ recoil mass from data with the MC simulated signal shapes, and the results agree well with those in Table II.

V. SYSTEMATIC UNCERTAINTIES

In this analysis, the reconstruction of the photon or the π^0 is not required. The branching fractions are obtained from the ratio of the numbers of events in the ranges defined above, so many of the systematic uncertainties related to the $D^0\bar{D}^0$ reconstruction, such as the tracking efficiencies, particle identification efficiencies, etc., cancel.

We use $M_{\text{Recoil}_{D^0\bar{D}^0}}^2 = 0.01$ (GeV/ c^2)² as the dividing

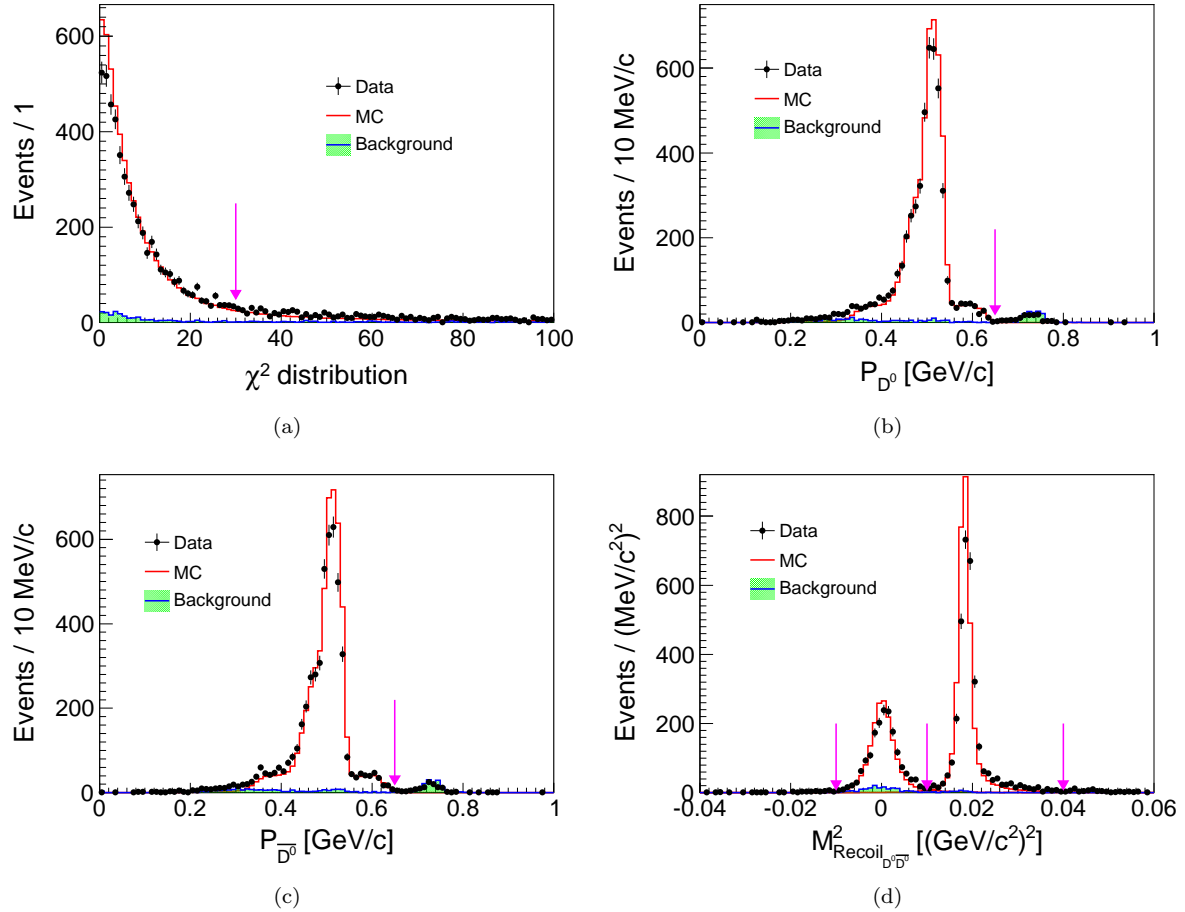


FIG. 1. Comparisons between data and MC simulation, summing the five modes listed in Table I: (a) the χ^2 distribution, (b) the momentum of D^0 , (c) the momentum of \bar{D}^0 , and (d) the square of the $D^0\bar{D}^0$ recoil mass. Dots with error bars are data, the open red histograms are MC simulations, and the filled green histograms are background events from the inclusive MC sample. The signal MCs are normalized to data according to the number of events, and background events from inclusive MC sample are normalized to data by luminosity.

TABLE II. Numbers used for the calculation of the branching fractions and the results. \mathcal{B}_{π^0} and \mathcal{B}_γ are the the branching fractions of $D^{*0} \rightarrow D^0\pi^0$ and $D^{*0} \rightarrow D^0\gamma$, respectively. “Combined” is the result obtained by summing the number of events for the five modes together; “weighted” averaged is the result from averaging the results from the five modes by taking the error in each mode as weighted factor. The uncertainties are statistical only.

Mode	$N_{\pi^0}^{\text{obs}}$	N_γ^{obs}	$N_{\pi^0}^{\text{bkg}}$	N_γ^{bkg}	$\epsilon_{\pi^0\pi^0}$ (%)	$\epsilon_{\gamma\gamma}$ (%)	$\epsilon_{\pi^0\gamma}$ (%)	$\epsilon_{\gamma\pi^0}$ (%)	\mathcal{B}_{π^0} (%)	\mathcal{B}_γ (%)
I	504 ± 23	281 ± 17	4 ± 2	24 ± 5	36.19	35.22	0.11	0.99	65.2 ± 1.9	34.8 ± 1.9
II	831 ± 29	419 ± 21	5 ± 2	36 ± 6	15.54	14.46	0.47	0.65	67.8 ± 1.6	32.2 ± 1.6
III	780 ± 28	441 ± 21	6 ± 3	38 ± 6	15.37	14.60	0.43	0.51	65.4 ± 1.6	34.6 ± 1.6
IV	538 ± 24	301 ± 18	10 ± 3	30 ± 6	19.04	18.34	0.09	0.51	65.1 ± 1.9	34.9 ± 1.9
V	518 ± 23	320 ± 18	11 ± 3	35 ± 6	19.05	18.48	0.11	0.53	63.2 ± 1.9	36.8 ± 1.9
Combined									65.7 ± 0.8	34.3 ± 0.8
Weighted average									65.5 ± 0.8	34.5 ± 0.8

line between $D^{*0} \rightarrow D^0\pi^0$ and $D^{*0} \rightarrow D^0\gamma$, as shown in Fig. 1(d). The systematic uncertainty due to this selection is estimated by comparing the branching frac-

tions via changing this requirement from 0.01 to 0.008 or 0.012 $(\text{GeV}/c^2)^2$.

The $D^{*0} \rightarrow D^0\pi^0$ and $D^{*0} \rightarrow D^0\gamma$ signal regions in

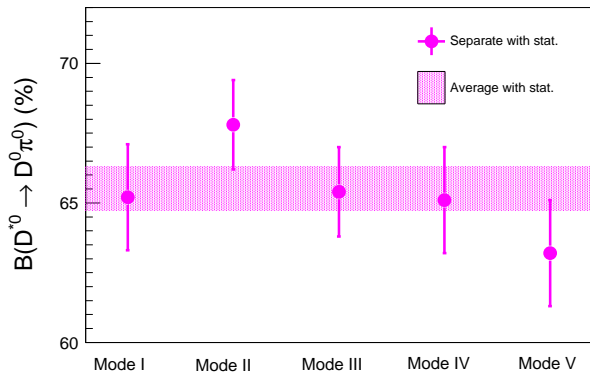


FIG. 2. The branching fraction of $D^{*0} \rightarrow D^0\pi^0$. The dots with error bars are the results from the five modes; the band represents the weighted average. Only statistical uncertainties are included.

the $D^0\bar{D}^0$ recoil mass squared spectrum are in the combined range of $[-0.01, 0.04]$ $(\text{GeV}/c^2)^2$; the associated systematic uncertainty is estimated by removing this requirement.

The corrected track parameters are used in the nominal MC simulation according to the procedure described in Ref. [21], and the difference in the branching fractions measured with and without this correction are taken as the systematic uncertainty caused by the requirement on the χ^2 of the kinematic fit.

The fraction of events with final state radiation (FSR) photons from charged pions in data is found to be 20% higher than that in MC simulation [22], and the associated systematic uncertainty is estimated by enlarging the ratio of FSR events in MC simulation by a factor of 1.2^X , where X is the number of charged pion in the final state, and taking the difference in the final result as systematic uncertainty.

The number of background events is calculated from the inclusive MC sample; the corresponding systematic uncertainty is estimated from the uncertainties of cross sections used in generating this sample. The dominant background events are from open charm processes and ISR production of $\psi(3770)$ with subsequent $\psi(3770) \rightarrow D^0\bar{D}^0$. The cross section for open charm processes is 7.1 nb, with an uncertainty of 0.31 nb or about 5% [7]. The cross section for ISR production of $\psi(3770)$ is 0.114 nb, with an uncertainty of 0.011 nb or about 9% which is calculated by varying Γ_{ee} and Γ_{total} of $\psi(3770)$ by 1σ . The systematic uncertainty related to the number of background events is conservatively estimated by changing the background level in Table II by 10% (larger than 5% and 9% mentioned above).

The efficiency in Table II is calculated using 200,000 signal MC events for each mode, but only the ratio of the efficiencies for $D^{*0} \rightarrow D^0\pi^0$ and $D^{*0} \rightarrow D^0\gamma$ is needed

in the branching fraction measurement. The systematic error caused by the statistical uncertainty of the MC samples is estimated by varying the efficiency for $D^{*0} \rightarrow D^0\gamma$ by 1σ of its statistical uncertainty, and the difference of the branching fraction is taken as the systematic uncertainty.

Other possible systematic uncertainty sources, such as from the simulation of ISR, the requirement on the charmed meson momentum, and the tracking efficiency difference caused by the tiny phase space difference between the two decay modes of D^{*0} , are investigated and are negligible.

The summary of the systematic uncertainties considered is shown in Table III. Assuming the systematic uncertainties from the different sources are independent, the total systematic uncertainty is found to be 0.5% by adding all the sources in quadrature.

TABLE III. The summary of the absolute systematic uncertainties in $\mathcal{B}(D^{*0} \rightarrow D^0\pi^0)$ and $\mathcal{B}(D^{*0} \rightarrow D^0\gamma)$.

Source	(%)
Dividing line between $D^{*0} \rightarrow D^0\pi^0$ and $D^{*0} \rightarrow D^0\gamma$	0.2
Choice of signal regions	0.2
Kinematic fit	0.2
FSR simulation	0.1
Background	0.2
Statistics of MC samples	0.2
Sum	0.5

VI. SUMMARY

By assuming that there are only two modes of D^{*0} , we measure the branching fractions of D^{*0} to be $\mathcal{B}(D^{*0} \rightarrow D^0\pi^0) = (65.5 \pm 0.8 \pm 0.5)\%$ and $\mathcal{B}(D^{*0} \rightarrow D^0\gamma) = (34.5 \pm 0.8 \pm 0.5)\%$, where the first uncertainties are statistical and the second ones are systematic. It should be noted that both the statistical and the systematic uncertainties of these two branching fractions are fully anti-correlated. Taking the correlations into account, the branching ratio $\mathcal{B}(D^{*0} \rightarrow D^0\pi^0)/\mathcal{B}(D^{*0} \rightarrow D^0\gamma) = 1.90 \pm 0.07 \pm 0.05$ is obtained. This ratio does not depend on any assumptions in the D^{*0} decays, so it can be used in calculating the D^{*0} decay branching fractions if more decay modes are discovered.

Figure 3 shows a comparison of the measured branching fraction of $D^{*0} \rightarrow D^0\pi^0$ with other experiments and the world average value [12]. Our measurement is consistent with the previous ones within about 1σ but with much better precision. These much improved results can be used to update the parameters in the effective models mentioned above, such as the mass of the charm

quark [3, 5], the effective coupling constant [4], and the magnetic moment of the charm quark [6]. With these new results as input, the uncertainty in the semileptonic decay branching fraction of B^\pm [8] can be reduced, thus leading to a tighter constraint on the standard model (SM) and its extensions.

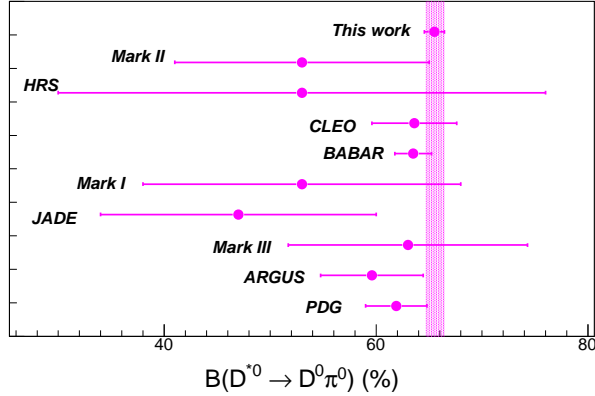


FIG. 3. Comparison of the branching fraction of $D^{*0} \rightarrow D^0\pi^0$ from this work and from previous experiments. Dots with error bars are results from different experiments, and the band is the result from this work with both statistical and systematic uncertainties.

ACKNOWLEDGMENTS

The BESIII collaboration thanks the staff of BEPCII and the IHEP computing center for their strong support. This work is supported in part by National Key Basic Research Program of China under Contract No. 2015CB856700; Joint Funds of the National Natural Science Foundation of China under Contracts Nos. 11079008, 11179007, U1232201, U1332201; National Natural Science Foundation of China (NSFC) under Contracts Nos. 10935007, 11121092, 11125525, 11235011, 11322544, 11335008; the Chinese Academy of Sciences (CAS) Large-Scale Scientific Facility Program; CAS under Contracts Nos. KJCX2-YW-N29, KJCX2-YW-N45; 100 Talents Program of CAS; INPAC and Shanghai Key Laboratory for Particle Physics and Cosmology; German Research Foundation DFG under Contract No. Collaborative Research Center CRC-1044; Istituto Nazionale di Fisica Nucleare, Italy; Ministry of Development of Turkey under Contract No. DPT2006K-120470; Russian Foundation for Basic Research under Contract No. 14-07-91152; U.S. Department of Energy under Contracts Nos. DE-FG02-04ER41291, DE-FG02-05ER41374, DE-FG02-94ER40823, DESC0010118; U.S. National Science Foundation; University of Groningen (RuG) and the Helmholtzzentrum fuer Schwerionenforschung GmbH (GSI), Darmstadt; WCU Program of National Research Foundation of Korea under Contract No. R32-2008-000-10155-0.

-
- [1] H. Fritzsch, M. Gell-Mann and H. Leutwyler, Phys. Lett. B **47**, 365 (1973).
- [2] N. Brambilla *et al.*, Eur. Phys. J. C **74**, 2981 (2014).
- [3] E. Eichten, K. Gottfried, T. Kinoshita, K. D. Lane and T. -M. Yan, Phys. Rev. D **21**, 203 (1980).
- [4] H. -Y. Cheng, C. -Y. Cheung, G. -L. Lin, Y. C. Lin, T. -M. Yan and H. -L. Yu, Phys. Rev. D **49**, 2490 (1994).
- [5] T. M. Aliev, E. Iltan and N. K. Pak, Phys. Lett. B **334**, 169 (1994).
- [6] G. A. Miller and P. Singer, Phys. Rev. D **37**, 2564 (1988).
- [7] D. Cronin-Hennessy *et al.* [CLEO Collaboration], Phys. Rev. D **80**, 072001 (2009).
- [8] A. Bozek *et al.* [Belle Collaboration], Phys. Rev. D **82**, 072005 (2010).
- [9] F. Butler *et al.* [CLEO Collaboration], Phys. Rev. Lett. **69**, 2041 (1992).
- [10] H. Albrecht *et al.* [ARGUS Collaboration], Z. Phys. C **66**, 63 (1995).
- [11] B. Aubert *et al.* [BaBar Collaboration], Phys. Rev. D **72**, 091101 (2005).
- [12] K. A. Olive *et al.* [Particle Data Group], Chin. Phys. C **38**, 090001 (2014).
- [13] M. Ablikim *et al.* [BESIII Collaboration], Nucl. Instrum. Meth. A **614**, 345 (2010).
- [14] S. Jadach, B. F. L. Ward and Z. Was, Comput. Phys. Commun. **130**, 260 (2000); S. Jadach, B. F. L. Ward and Z. Was, Phys. Rev. D **63**, 113009 (2001).
- [15] D. J. Lange, Nucl. Instrum. Meth. A **462**, 152 (2001); R. G. Ping, Chin. Phys. C **32**, 599 (2008).
- [16] J. C. Chen, G. S. Huang, X. R. Qi, D. H. Zhang and Y. S. Zhu, Phys. Rev. D **62**, 034003 (2000).
- [17] T. Sjostrand, S. Mrenna and P. Z. Skands, JHEP **0605**, 026 (2006).
- [18] S. Agostinelli *et al.* [GEANT4 Collaboration], Nucl. Instrum. Meth. A **506**, 250 (2003).
- [19] J. Allison, K. Amako, J. Apostolakis, H. Araujo, P. A. Dubois, M. Asai, G. Barrand and R. Capra *et al.*, IEEE Trans. Nucl. Sci. **53**, 270 (2006).
- [20] D. Guetta and P. Singer, Phys. Rev. D **61**, 054014 (2000).
- [21] M. Ablikim *et al.* [BESIII Collaboration], Phys. Rev. D **87**, 012002 (2013).
- [22] M. Ablikim *et al.* [BESIII Collaboration], Phys. Rev. D **84**, 091102 (2011).